

# An on-site preparable, novel bone-grafting complex consisting of human platelet-rich fibrin and porous particles made of a recombinant collagen-like protein

Tsuneyuki Tsukioka,<sup>1†</sup> Takahiro Hiratsuka,<sup>2†</sup> Masayuki Nakamura,<sup>1</sup> Taisuke Watanabe,<sup>1</sup> Yutaka Kitamura,<sup>1</sup> Kazushige Isobe,<sup>1</sup> Toshimitsu Okudera,<sup>1</sup> Hajime Okudera,<sup>1</sup> Akihiko Azuma,<sup>2</sup> Kohya Uematsu,<sup>3</sup> Koh Nakata,<sup>4</sup> Tomoyuki Kawase<sup>5</sup>

<sup>1</sup>Tokyo Plastic Dental Society, Tokyo, Japan

<sup>2</sup>Bioscience & Technology Development Center, FUJIFILM Corporation, Kanagawa, Japan

<sup>3</sup>Division of Implantology, Niigata University Medical and Dental Hospital, Niigata, Japan

<sup>4</sup>Bioscience Medical Research Center, Niigata University Medical and Dental Hospital, Niigata, Japan

<sup>5</sup>Division of Oral Bioengineering, Institute of Medicine and Dentistry, Niigata University, Niigata, Japan

Received 13 February 2018; revised 13 June 2018; accepted 18 August 2018

Published online 00 Month 2018 in Wiley Online Library (wileyonlinelibrary.com). DOI: 10.1002/jbm.b.34234

**Abstract:** Platelet-rich fibrin (PRF) is widely used in regenerative medicine. Nonetheless, major issues include its controversial effects on bone regeneration and a lack of quality-assured glass tubes required for coagulation. We used porous particles (FBG) comprising a recombinant RGD motif-enriched collagen I-like protein to activate the coagulation pathway and examined the effects of the resulting PRF–FBG complex on bone regeneration. Human whole-blood samples were mixed with FBG in plastic tubes and centrifuged to prepare a PRF–FBG complex. Platelet-derived growth factor-BB (PDGF-BB) levels and cell growth activity were determined by ELISA and a bioassay using osteoblasts. Bone regenerative activity was assessed using a mouse model of calvarial bone defect. FBG facilitated PRF-like matrix formation during centrifugation. In this PRF–FBG complex, the microstructure of fibrin fibers was

similar to that of PRF prepared conventionally in glass tubes. PDGF-BB levels and mitogenic action were not significantly influenced by FBG. In the bone defect model, although PRF did not exert any significant positive effects on its own, in combination with FBG, it synergistically stimulated new bone formation. This study demonstrated that incorporation of FBG into whole-blood samples induces PRF formation without the aid of glass tubes. The resulting PRF–FBG complex could be a promising bone grafting material in clinical settings. © 2018 The Authors. Journal Of Biomedical Materials Research Part B: Applied Biomaterials Published By Wiley Periodicals, Inc J Biomed Mater Res B Part B: 00B: 000–000, 2018.

**Key Words:** bone grafting material, platelet-rich fibrin, collagen-like protein, RGD motif, calvarial bone defect, coagulation

**How to cite this article:** Tsukioka T, Hiratsuka T, Nakamura M, Watanabe T, Kitamura Y, Isobe K, Okudera T, Okudera H, Azuma A, Uematsu K, Nakata K, Kawase T. 2018. An on-site preparable, novel bone-grafting complex consisting of human platelet-rich fibrin and porous particles made of a recombinant collagen-like protein. J Biomed Mater Res B Part B 2018;9999:9999:1–11.

## INTRODUCTION

A major characteristic of the bioresorbable biomaterial called recombinant protein (RCP) developed for medical applications by FUJIFILM (Tokyo, Japan) is that 12 RGD (Arg–Gly–Asp) motifs of the  $\alpha 1$  sequence of human type I collagen are present in a single molecule.<sup>1,2</sup> Thus, sodium dodecyl sulfate polyacrylamide gel electrophoresis (SDS-PAGE) shows a single band at 51 kDa. Because this protein does not contain sequences of an antigenic telopeptide or animal-derived components, it is thought to be safer than various commercially available collagen products derived from bovine or pig

collagen. In addition, RCP is a recombinant protein produced by the yeast *Pichia pastoris* and differs from conventional animal collagen because there is no risk of infection, such as bovine spongiform encephalopathy.<sup>1</sup>

The porous particles used in this study, which are designated as FBG, are prepared by freeze-drying a solution of the protein. Acute toxicity of this product has not been observed in various cultured cells and animal models in either Good Laboratory Practices (GLP) or non-GLP grade verification procedures (personal communication, FUJIFILM). As for other advantages, this protein can degrade at an

Additional Supporting Information may be found in the online version of this article.

<sup>†</sup>These authors contributed equally to this work.

**Correspondence to:** T. Kawase; e-mail: kawase@dent.niigata-u.ac.jp

This is an open access article under the terms of the Creative Commons Attribution-NonCommercial License, which permits use, distribution and reproduction in any medium, provided the original work is properly cited and is not used for commercial purposes.

implantation site as animal-derived collagen sponges, and its stiffness maintains porous structure even after wetting, thereby allowing surrounding cells to easily invade the deep pores.<sup>1</sup> The latter advantage is also expected to function as a spacer in a bone defect to support bone regeneration. To date, no apparent disadvantages have been found.

Platelet-rich fibrin (PRF) is a modification of platelet-rich plasma (PRP) and is prepared by exclusion of anticoagulants and coagulation factors; PRF is widely used in various fields of regenerative therapy. Its clinical use is essentially based on the evidence that PRF contains high concentrations of growth factors and a well-cross-linked dense fibrin mesh.<sup>3</sup> Nevertheless, it has been debated whether PRF is effective at regenerating a skeletal tissue.<sup>4–7</sup> In addition to the wide variation in characteristics of individual PRF samples and host site conditions, a possible explanation for the less reproducible outcomes could be PRF's degradability: PRF is degraded in gingival connective tissue generally within 10 days post-implantation.<sup>8</sup> Therefore, to improve PRF's capacity for bone regeneration, it is necessary to find a way to prolong the lifetime of PRF and controlled release of growth factors at implantation sites.

Recently, PRF has been facing another issue. It is a practical issue, namely, discontinued supply of disposable glass tubes for blood collection. For ecological reasons, world's major manufacturers of medical equipment had decided to no longer produce glass tubes for blood collection.<sup>9</sup> It is well known that glass surface triggers blood coagulation through activation of coagulation factor XII.<sup>10,11</sup> When glass tubes are replaced with plastic ones, blood samples hardly clot within 30 min.<sup>12</sup> For many embarrassed end users, doctors, and dentists in Japan, several distributors have ordered glass tubes from foreign subcontract factories or recommend the customers to use plastic tubes coated with a silica film or microscopic silica particles for coagulation testing. To date, no one has demonstrated the safety of these products for PRF therapy. These products are developed and supplied solely for routine laboratory analyses, not for preparation of blood-derived products that are implanted into the human body.<sup>13</sup> Therefore, many users are now facing a risky situation where they consciously or subconsciously employ the products that are not guaranteed to be suitable for regenerative therapy.

To solve these problems, we have looked for appropriate biomaterials and chose porous, collagen I-like protein based particles, FBG. We expected that FBG's abundant RGD motif activates platelets to trigger coagulation without the aid of a glass surface or any exogenous coagulation factors. We also hypothesized that PRF, when combined with FBG, will become resistant to biodegradation. In this study, we investigated the complex matrix of PRF with FBG and validated its applicability as a bone-grafting material.

## MATERIALS AND METHODS

### Preparation of FBG

After freeze-drying, RCP blocks were cross-linked via a heat-dependent dehydration condensation reaction and crushed into particles (FBG).<sup>14</sup> Porosity was estimated at 70%–95% by a mercury intrusion porosimeter. Biodegradation and

mechanical strength can be controlled by modifying cross-link density.<sup>14</sup> Unlike many commercially available collagen sponges, such as Terudermis (Olympus-Terumo Biomaterials, Tokyo, Japan), FBG tested in this study can maintain its porous structure in a liquid.<sup>14</sup>

### Preparation of PRP and clot formation under the influence of added CaCl<sub>2</sub>

Blood samples were collected from eight nonsmoking healthy male volunteers at ages 32–68 years. The study design and consent forms for all the procedures performed were approved by the ethics committee for human participants of the Niigata University School of Medicine (Niigata, Japan) in accordance with the Helsinki Declaration of 1964 as revised in 2013.

Peripheral blood (~9 mL) was collected into plastic vacuum plain blood collection tubes (Neotube; NIPRO, Osaka, Japan) containing 1 mL of the A-formulation of acid-citrate-dextrose (ACD-A; Terumo, Tokyo, Japan), and was immediately centrifuged at 530*g* for 10 min. The upper plasma fraction was collected, transferred to fresh tubes, and served as a PRP fraction.<sup>15,16</sup> The number of platelets and other blood cells in whole-blood samples and PRP preparations was determined on an automated hematology analyzer (poch 100iV, Sysmex, Kobe, Japan).

After addition of 0.1% CaCl<sub>2</sub>, PRP fractions were incubated at 37°C on watch glasses or plastic dishes in the presence or absence of FBG. Time needed for complete clotting was determined.

### Preparation of FBG- or Terudermis-containing plastic tubes

FBG samples were subdivided into three groups: (a) a non-fractionated group, (b) small-size (425–500 μm) group, and (c) medium-size (500–710 μm) group. Into each plastic tube (Venoject II; Terumo), 22–28 mg of one of three types of FBG was added. Terudermis (Olympus-Terumo Biomaterials)<sup>17</sup> was cut into small pieces (~1 × 1 × 1 mm) and 13–22 mg of cut up Terudermis was added into plastic tubes.

### Preparation of PRF and PRF-like matrices

For preparing control PRF, fresh whole-blood samples were collected into glass tubes (BD Vacutainer blood collection tube; Becton Dickinson and Company, Franklin Lakes, NJ) in the absence of ACD-A and were immediately centrifuged by means of a Medifuge centrifugation system (Silfradent S.r.l., Santa Sofia, Italy). This centrifuge was designed to prepare concentrated growth factors (CGF, which may be considered a member of the PRF family) and is controlled by a program that automatically changes the centrifugal speed as follows: 30'', acceleration; 2', 692*g*; 4', 547*g*; 4', 592*g*; 3', 855*g*; and 36'', deceleration and stop.<sup>15</sup> Nevertheless, we classify CGF into the PRF family and therefore use "PRF" as CGF's generic name in this study as proposed in a recent article.<sup>18</sup>

For mixing with FBG or pieces of Terudermis, whole-blood samples freshly collected into plastic tubes (Venoject II) were transferred into the tubes containing those materials and gently mixed by inverting for 5 min prior to

centrifugation. The PRF-like matrix was prepared by means of the centrifuge as described above.

The resulting PRF and PRF-like matrices were immediately compressed with a stainless-steel PRF compression device (PRF stamper; JMR Corp. Ltd., Niigata, Japan)<sup>19</sup> to drain excess amounts of exudates and were washed thrice with PBS for scanning electron microscopy (SEM) or stored without washing at  $-80^{\circ}\text{C}$  until determination of PDGF-BB levels.

In this study, the amount of FBG particles in a tube was optimized for the size of the bone defect (see the section of “animal implantation study”) without compromising the efficiency of clot formation.

### Scanning electron microscopic examination of fibrin clot and platelets

After washing, individual PRF and PRF-like clots were fixed with 2.5% neutralized glutaraldehyde, serially dehydrated in ethanol and *t*-butanol solutions, and freeze dried. These samples were then examined under a scanning electron microscope (TM-1000; Hitachi, Tokyo, Japan) at an accelerating voltage of 15 kV, as described previously.<sup>20,21</sup>

Fibrin fibers were randomly selected in SEM images and measured manually, using a scale ( $N = 8$ ).

### Quantitation of PDGF-BB by ELISA

Individual frozen whole PRF or PRF-like matrices were minced with scissors and homogenized for 1 min with sample tube size disposable homogenizers (BioMasher II; Nippi, Tokyo, Japan). After high-speed centrifugation (7,340g), the resulting supernatants (i.e., PRF extracts) of the homogenates were subjected to PDGF-BB assay using the Human PDGF-BB Quantikine ELISA Kit (R&D Systems, Inc., Minneapolis, MN) as previously described.<sup>22–24</sup>

### A cell proliferation assay

With informed consent, human periosteum tissue segments were aseptically excised from the periodontal tissue on the healthy buccal side of the retromolar region in the mandibles of two nonsmoking female volunteers (age 19 and 29). Human-alveolar-bone-derived periosteal cell sheets were prepared by explant cultivation of the periosteum tissue pieces and were dispersed with 0.05% trypsin plus 0.53 mM EDTA (Invitrogen, Carlsbad, CA) to release single cells, as described previously.<sup>22,25,26</sup> The periosteal cells were seeded at a density of  $0.4 \times 10^3$  per well in 24-well plates and were precultured in DMEM containing 1% of fetal bovine serum (FBS; Invitrogen, Carlsbad, CA) for 24 h.

Next, the cells were treated with 1% PRF extracts, which were prepared as described in the above section, for 72 h in DMEM containing 1% of FBS. Three different lots of PRF extracts and three batches of human periosteal cells were used for each experiment. At the end of the incubation periods, periosteal cells were harvested using 0.05% trypsin plus 0.53 mM EDTA and immediately counted on an automated cell counter (Moxi-z; ORLFO Technologies, Ketchum, ID) ( $N = 12$ ).<sup>22</sup> Human osteoblastic Saos-2 ( $N = 8$ ) and immature osteoblastic MG63 cells ( $N = 6$ )<sup>27,28</sup> were treated

with the PRF extract and cell proliferation was evaluated as described above.

### An animal implantation experiment

ICR-nu/nu mice (male, age: 4–5 weeks old, weight: 19–27 g) were obtained from Japan Charles River Laboratories (Yokohama, Japan) and housed at the Bioscience & Technology Development Center of FUJIFILM Corp. at least 1 week prior to the experiment.

The mice were placed in a chamber and exposed to a gas mixture of 4% isoflurane to induce anesthesia. During the surgical procedure, the mice were anesthetized by inhalation of 2% isoflurane via a tube. The surface of the surgical site was disinfected with a povidone iodine solution before the operation. For implantation, bone defects of critical size ( $\emptyset$  3 mm) were made on a calvaria using a trephine bur and filled with simple PRF or PRF–Terudermis complex or PRF–FBG complex matrices, essentially as described elsewhere.<sup>29</sup>

The care and use of the animals complied with the Guiding Principles for the Care and Use of Animals, as approved by Niigata University.

### Histopathological examination

Nude mice were euthanized at 2 ( $N = 3$ –4) or 4 weeks ( $N = 5$ ) postimplantation. For histopathological examination, the calvariae of the mice were then collected and fixed with 4% neutral-buffered paraformaldehyde, then decalcified with 10% formic acid, dehydrated, embedded in paraffin, sectioned for staining, and sectioned sagittally at thickness 3  $\mu\text{m}$ . Each slice was stained with hematoxylin and eosin (H&E).

Quantitative analysis of images of newly formed bone area in the defect was performed in the ImageJ software (NIH, Bethesda, MD). The images of sections were transformed from the color mode into binary mode. When histopathological images were transformed into binary images, the boundary between newly formed bone area and other areas was determined carefully.

### Statistical analysis

The data were expressed as mean  $\pm$  standard deviation (SD). For multigroup comparisons, statistical analyses were conducted to compare the mean values by one-way analysis of variance (ANOVA), followed by Tukey’s multiple-comparison test (SigmaPlot 12.5; Systat Software, Inc., San Jose, CA). Differences with *p* values of  $<0.05$  were considered statistically significant.

## RESULTS

### PRF-like fibrin clot formation under the influence of FBG

Fibrin clot formation using the PRP fraction is shown in Figure 1. The citrated PRP fraction was mixed with  $\text{CaCl}_2$ , divided into samples for a watch glass and for a plastic dish, one of which contained FBG particles, and was incubated at  $37^{\circ}\text{C}$ . The ranking of clot formation rates was “plain watch glass”  $>$  “plastic dish with FBG”  $>$  “plain plastic dish,” while the ranking of clot size was “plastic dish with FBG”  $\geq$  “plain watch glass”  $\gg$  “plain plastic dish.”

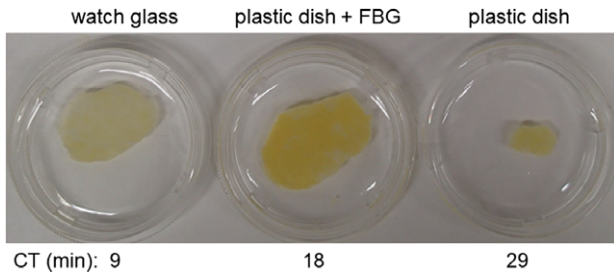
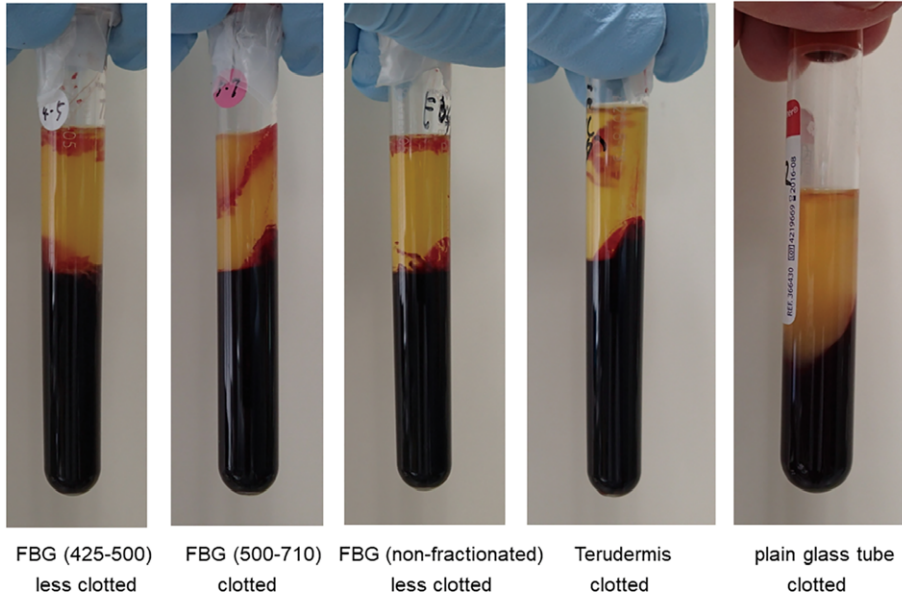


**FIGURE 1.** Comparisons of size and clotting time among PRP-derived fibrin clots. Citrated liquid PRP fractions (1.5 mL) were mixed with 0.1% CaCl<sub>2</sub> on a watch glass or plastic dishes in the absence or presence of FBG. The resulting clots were compressed, washed, and fixed in a 10% neutralized formalin solution for 10 min in 35 mm plastic dishes. Similar results were obtained from three other samples collected from different donors.

PRF-like fibrin matrix formation from fresh whole-blood samples is illustrated in Figure 2. In plastic tubes, both Terudermis and FBG, irrespective of particle size, formed PRF-like clots similar to those in plain glass tubes. Nonetheless, additional centrifugation was sometimes required for Terudermis- or FBG-dependent clot formation when clot formation was incomplete under relatively lower ambient temperature. However, no apparent macroscopic differences were detected in clot size. Furthermore, no substantial differences in platelet aggregates or fibrin fibers were founded among fractionated and nonfractionated FBG groups. However, because of somewhat higher efficacy and reproducibility, medium-size FBG particles were used in the following experiments.

The appearance of the PRF-like matrix was categorized into three regions and SEM observations of the upper regions

(A) Just after centrifugal fractionation



(B) After trimming red thrombi

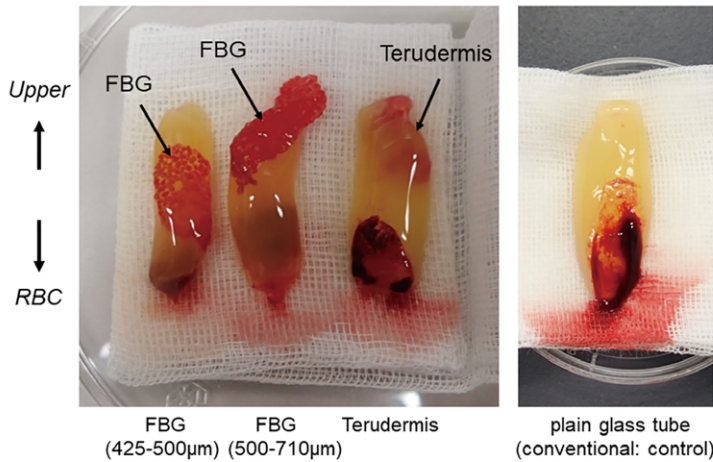


**FIGURE 2.** A: Appearances of fractionated whole-blood samples in plastic tubes with FBG or Terudermis or in a glass tube and the resulting PRF or PRF-like clots. B: Appearances of trimmed PRF and PRF-like clots prepared above. The numbers in parentheses after FBG represent the size of FBG particles in micrometers.

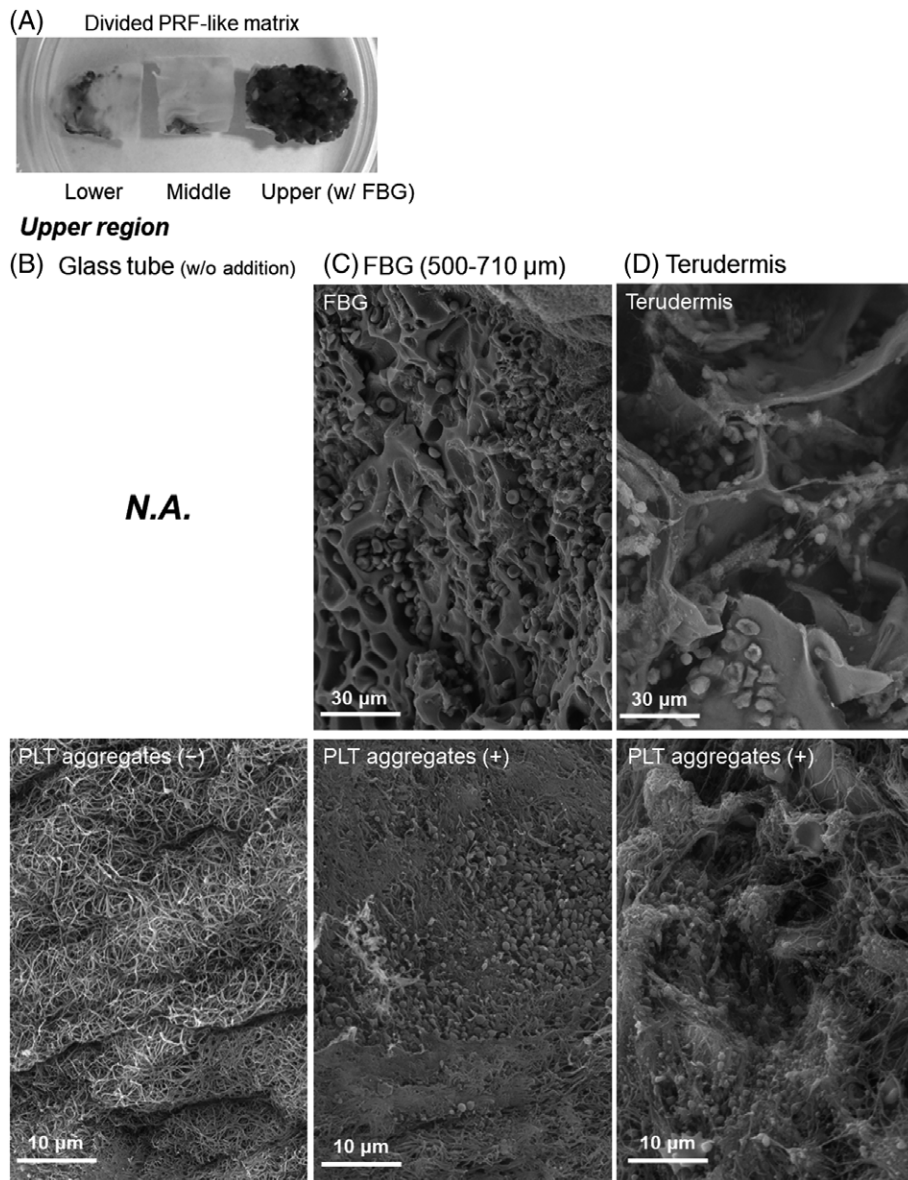


**FIGURE 3.** An appearance of PRF-like matrix divided into three regions and SEM observations of the upper regions of three PRF types. A: An FBG-dependent PRF-like matrix and a Terudermis-dependent PRF-like matrix and the control PRF matrix were divided into three regions (upper, middle, and lower). The length of PRF and PRF-like matrices ranged from  $\sim 40$  to  $50$  mm. B–D: Microstructures of surfaces of the resulting PRF and PRF-like clots prepared in glass tubes or in plastic tubes with FBG or Terudermis. B: A plain glass tube without any material. C: A plastic tube with FBG ( $500\text{--}710$   $\mu\text{m}$ ). D: A plastic tube with Terudermis ( $\sim 1 \times 1 \times 1$  mm). Upper and lower panels show materials added and platelet (PLT) aggregates, respectively. Note: in a glass tube, no materials were added and PLT aggregates were markedly decreased in the upper region.

of three PRF types are shown in Figure 3. The resulting PRF or PRF-like matrices were divided into three regions, as reported previously,<sup>21</sup> and subjected to the following SEM examination. Platelets attached almost equally on the surface of FBG and Terudermis particles. Although RGD motifs were enriched in FBG, the number of platelets attached on FBG particles were less numerous than expected and platelets did not aggregate together. Similar platelet aggregates were observed on the surface of these fibrin clots near the materials. In contrast, few platelet aggregates were detected in the upper region of the control PRF matrix.

SEM observations of platelet aggregates in the middle and the lower regions of three PRF types are shown in

Figure 4. Platelet aggregates, the distribution of which somewhat decreased by a gentle gradient from the upper to the lower region, were constantly distributed in both FBG- and Terudermis-dependent PRF-like matrices. In contrast, platelet aggregates were highly concentrated in the lower region of the control PRF matrix, as described previously.<sup>21</sup>

SEM observations of fibrin fibers in the middle regions of three PRF types are shown in Figure 5. In terms of thickness and cross-link density, a mesh-like arrangement of fibrin fibers was formed in an FBG-dependent PRF matrix and was similar to those of Terudermis-dependent PRF-like matrix and the control PRF matrix.

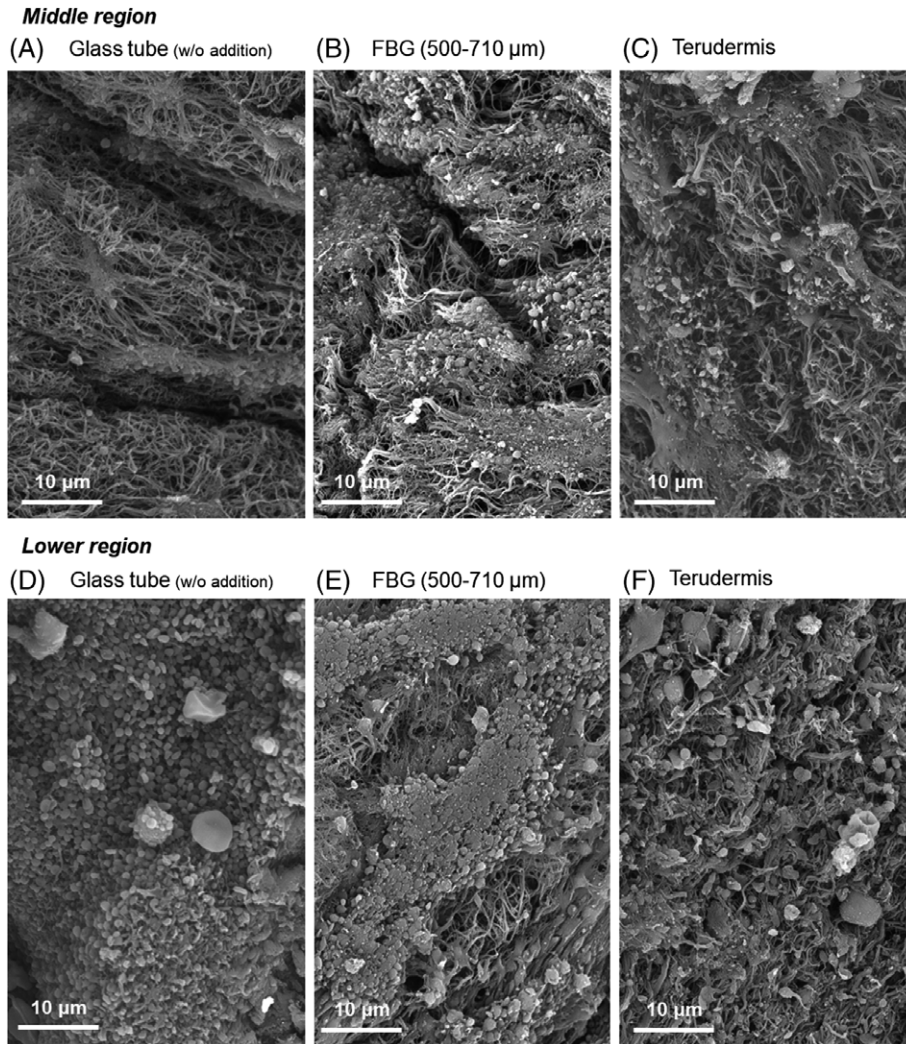


**FIGURE 4.** SEM observations of platelet aggregates in the middle and the lower regions of the three PRF types. A: A glass tube without any material. B: A plastic tube with FBG ( $\varnothing$ 500–710  $\mu\text{m}$ ). C: A plastic tube with Terudermis ( $\sim 1 \times 1 \times 1 \text{ mm}$ ). Upper and lower panels show the middle and the lower regions, respectively.

### Stimulatory effects of FBG on platelets

In the process of PRF-like clot formation, because platelets were attached on fibrin fibers and aggregated with one another, platelets were activated. To further demonstrate the

release of coagulation factors and growth factors from activated platelets, morphological changes in platelets were examined in the presence of FBG particles. Temporal SEM observations of platelet adhesion on FBG particles (control: plastic dishes) and microparticles blebbing on platelets are shown in Figure 6. Compared with PRF-like clot formation, presumably because of the lack of albumin, washed platelets attached on the FBG particles at seemingly higher densities [Figure 6(A–D)]. Upon continuous incubation on the nanoprecipitator filters, several platelets formed filopodial; however, overall, platelets were recognized at initial stages of activation in the control platelet suspension. In contrast, in the presence of FBG particles, several platelets formed lamellipodia and attached on the filter with an enlarged area. In addition, typical microparticles budding from platelets were detected in several aggregated platelets.

### Middle region

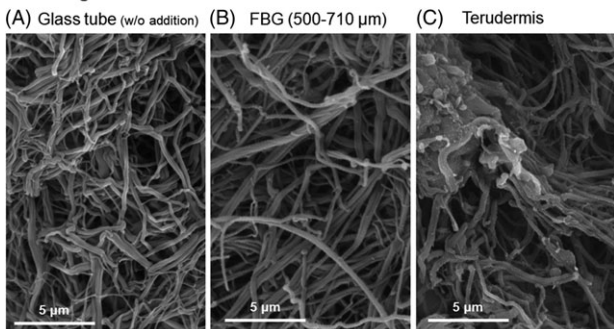


**FIGURE 5.** SEM observations of fibrin fibers in the middle regions of three PRF types. A: A glass tube without any material. B: A plastic tube with FBG ( $\varnothing$ 500–710  $\mu\text{m}$ ). C: A plastic tube with Terudermis ( $\sim 1 \times 1 \times 1 \text{ mm}$ ).

### Biological effects of PRF-like fibrin clots

To assess possible loss or “irreversible absorption” of growth factors, we determined PDGF-BB levels in individual extracts.

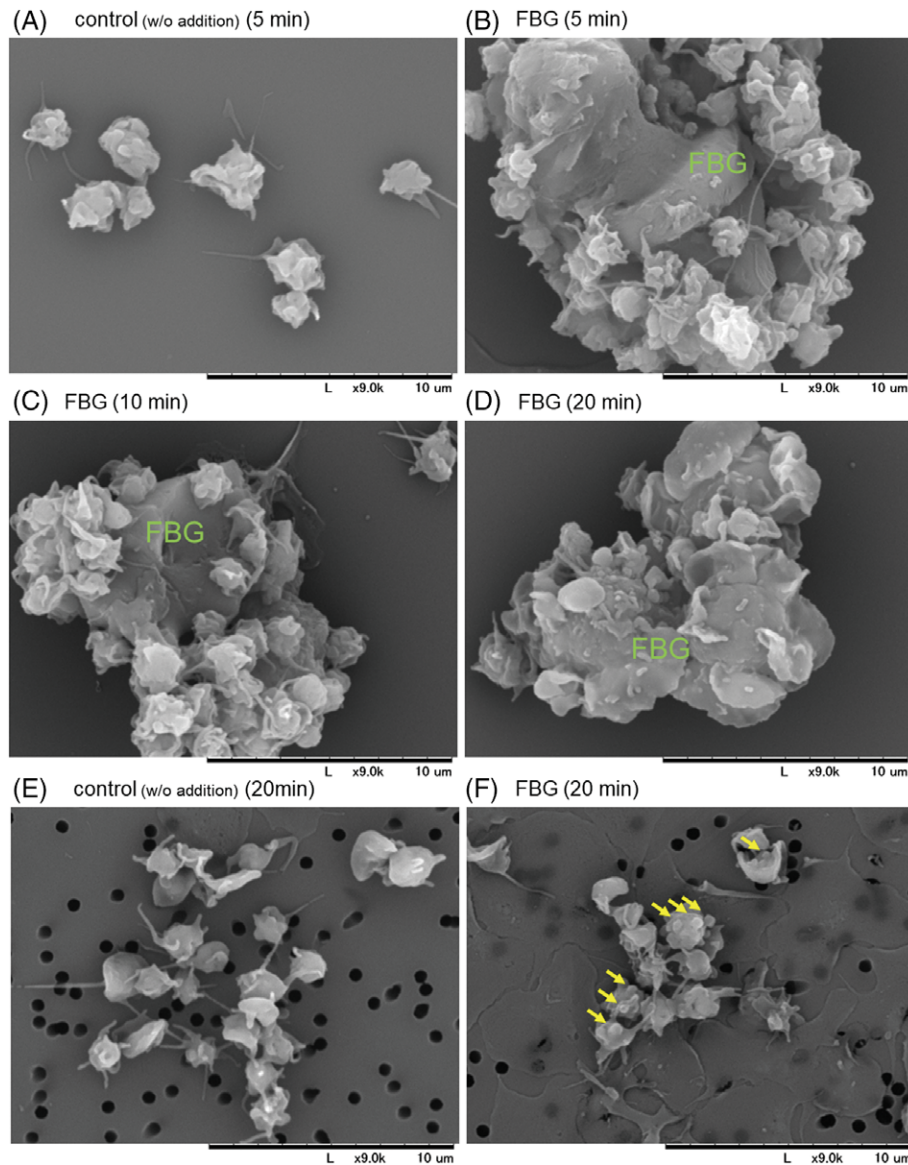


**FIGURE 6.** Temporal SEM observations of platelet adhesion on FBG particles (control: plastic dishes) and microparticles blebbing on platelets. A–D: Washed platelets were incubated with smaller FBG particles (<100 μm) in sample tubes for 5, 10, and 20 min and the mixtures were transferred into plastic dishes at 5 min before the end of the experiment. E,F: Washed platelets were incubated with FBG (Ø500–710 μm) for 20 min on nano-percolators. Yellow arrows indicate microparticles blebbing on platelets. These experiments were performed at ambient temperature.

PDGF-BB concentrations in the PRF clots that formed in glass tubes and those formed in plastic tubes that contained FBG or Terudermis are shown in Supporting Information, Figure S1(A). No significant differences were noted among these samples. Effects of individual PRF extracts on cell proliferation are shown in Supporting Information, Figure S1(B–D). In human primary periosteal cells, as well as in human osteoblastic Saos-2 and immature osteoblastic MG63 cells, no significant differences in mitogenic action were found among individual extracts.

Effects of PRF-like clots prepared by means of FBG or Terudermis on new bone formation in nude mice at 2 weeks post-implantation are shown in Figure 7. Microscopically undetectable levels of bone formation in calvarial bone defects were found in groups “control” and “PRF + Terudermis,” while

only slight bone formation was found in groups “PRF alone” and “FBG alone.” In the “PRF + FBG” group, active bone formation was found in deep pore regions. Image analysis revealed that the “PRF + FBG” complex most effectively and significantly induced bone formation as compared with the other groups.

Effects of PRF-like clots prepared by means of FBG and Terudermis on new bone formation in nude mice at 4 weeks postimplantation are shown in Figure 8. Additional 2 weeks observation indicated slightly increased bone formation in groups “control,” “PRF alone,” and “PRF + Terudermis” and significantly facilitated bone growth in groups “FBG alone” and “PRF + FBG.” Image analysis revealed that FBG alone had stimulatory effects on bone formation, and that PRF synergistically augmented FBG-induced bone formation. In contrast, “PRF + Terudermis” was less effective than FBG alone.

2 weeks post-implantation

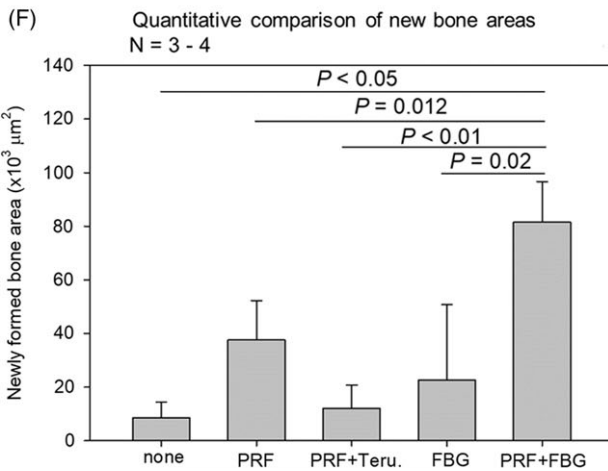
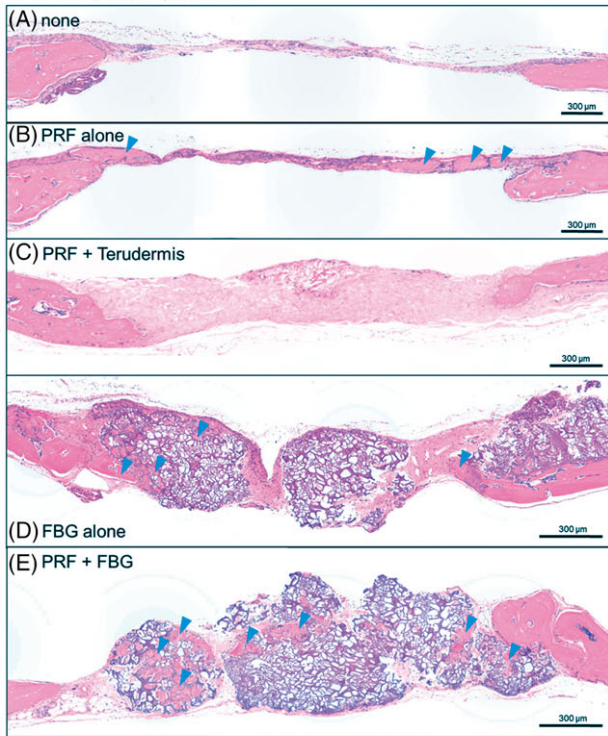


**FIGURE 7.** Effects of PRF clots on new bone formation in a nude-mouse model of a calvarial bone defect at 2 weeks postimplantation. A: None; B: PRF alone; C: PRF + Terudermis; D: FBG alone; E: PRF + FBG. Blue arrowheads indicate newly formed woven bone. F: Comparison of the areas of newly formed bone assessed by quantitative image analysis.  $N = 3-4$ .

Differences between individual effects were not statistically significant but reproducible in our experiment.

## DISCUSSION

The major outcomes of this study are validation of a glass-free plastic-based PRF clot formation system containing FBG and the potent effects of the resulting FBG-containing PRF clots on bone regeneration.

FUJIFILM Corporation, Tokyo, Japan developed a new bioresorbable biomaterial called RCP for medical applications and

demonstrated its biological utility.<sup>1,2</sup> In this study, we developed a PRF preparation system composed of a plastic tube and FBG derived from freeze-dried RCP and validated the usefulness of this product. We found that although often requiring a little longer period of preparation, this product enables preparing PRF as in a glass tube. Furthermore, the resulting PRF clots including FBG were very similar to the original PRF clots in *in vitro* studies, but these PRF clots showed higher capacity for new bone formation than the other types of PRF clots in the animal implantation experiment.

It is well known that a negatively charged glass surface induces coagulation via activation of coagulation factor XII. Therefore, freshly collected whole-blood samples even without any anticoagulants do not clot immediately within ~30 min. Nonetheless, in our previous study (manuscript submitted), we demonstrated that addition of an atelocollagen sponge is sufficient to induce clot formation of liquid PRP preparations via activation of platelets in plastic dishes. In this study, we expanded this finding to PRF preparation in plastic tubes.

The most plausible mechanism of platelet-dependent PRF clot formation can be explained as follows. In case of conventional glass tubes, activated XII triggers the intrinsic coagulation cascade and consequently forms fibrin clots without platelets. In contrast, in case of our newly developed system, activated platelets release microparticles containing kininogen, VIIIa, Va, prothrombin, and fibrinogen, and thereby act on several steps of the cascade to form fibrin clots. Although responses of platelets to FBG remains to be clarified in detail, the similar platelet-dependent coagulation mechanism is thought to be involved in Ca<sup>2+</sup>-induced coagulation of plasma rich in growth factors (PRGF) preparations: the lower plasma fraction (F2), which contains concentrated platelets, can be clotted by CaCl<sub>2</sub> substantially faster than can the upper plasma fraction (F1), which is free of platelets (personal communication, BTI Biotechnology Institute, Vitoria-Gasteiz, Spain).

In terms of the mechanism of platelet activation, platelets have two major receptors for collagen: integrin  $\alpha 2\beta 1$  and glycoprotein VI. On the other hand, platelets also express integrins  $\alpha 11\beta 3$ ,  $\alpha v\beta 3$ ,  $\alpha 5\beta 1$ , and  $\alpha 5\beta 1$  as minor collagen receptors, all of which can specifically bind to the RGD motif. Although the collagen sponge is thought to activate platelets through all these major and minor collagen receptors, we found no apparent differences between the collagen sponge and FBG in the time required for clot formation. Therefore, this finding suggests that these minor collagen receptors function together and in collaboration with the major receptors that drive platelet activation.

FBG alone reportedly stimulated bone formation in an animal experiment.<sup>14</sup> In this study, we confirmed the ability of FBG in a similar experiment on immune-deficient mice; this ability is believed to somewhat influence bone regeneration. The advantages of this collagen-like material include a more robust porous structure in comparison with other (conventional) collagen sponges, including Terudermis. These favorable effects of FBG and collagen on bone formation can be explained on the basis of their common



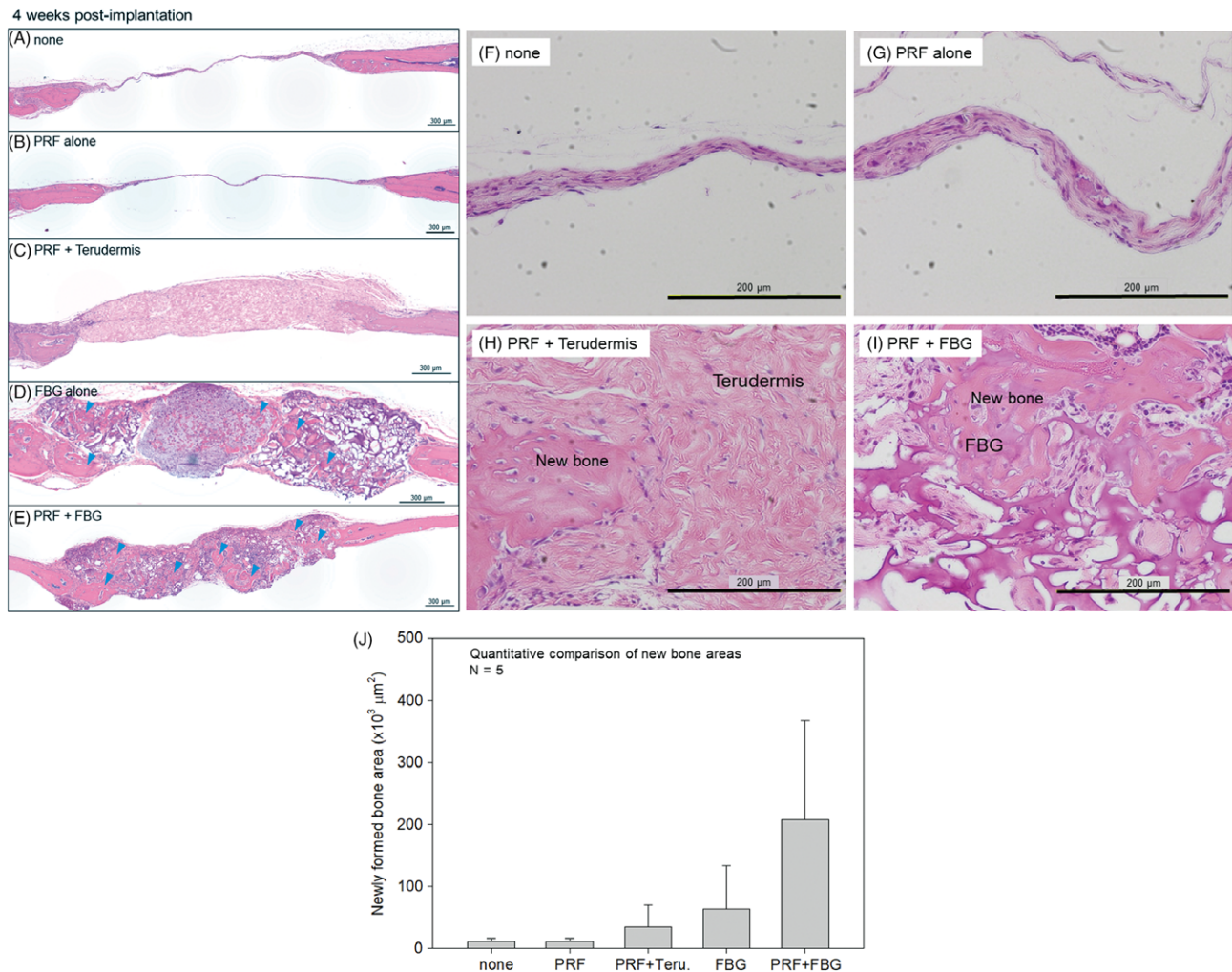


**FIGURE 8.** Effects of PRF clots on new bone formation in the nude-mouse model of the calvarial bone defect at 4 weeks postimplantation. A: None; B: PRF alone; C: PRF + Terudermis; D: FBG alone; E: PRF + FBG; F: None (greater magnification); G: PRF alone (greater magnification); H: PRF + Terudermis (greater magnification); I: PRF + FBG (greater magnification). Blue arrowheads indicate newly formed woven bone. J: Comparison of the areas of newly formed bone assessed by quantitative image analysis. No statistically significant differences were detected among these groups;  $N = 5$ .

characteristic: the RGD-motif can stimulate osteoblast adherence, proliferation, and differentiation.<sup>30–32</sup> In addition, probably as a remarkable advantage of this material, FBG particles provide relatively stiff pores, a microstructure that is suitable for blood capillaries, osteoblasts, and their precursor cells to easily invade and form a niche suitable for bone formation.

However, although we preliminarily hypothesized that PRF can stimulate bone regeneration by its enriched growth factors, we did not detect significant positive effects of PRF alone in this animal experiment. According to recent reports investigating the representative growth factors contained in PRP, which are common to PRF, both PDGF and TGF $\beta$  function as an osteoinductive factor to stimulate the proliferation and osteogenic differentiation of mesenchymal stem cells.<sup>33–36</sup> However, the effects of PRP or PRF on bone regeneration are still controversial in preclinical and clinical studies.<sup>37</sup> We believe that this discrepancy has probably arisen owing to the lack of quality analysis of individual PRP

or PRF preparations. The contents in PRP and PRF vary with individual samples and preparation protocols.<sup>24</sup> In this study, we employed a centrifugation-based protocol to prepare concentrated growth factors (CGF),<sup>18</sup> a particular brand name of the PRF family, which inevitably includes enriched leukocytes and related proinflammatory cytokines.<sup>24</sup> Leukocyte inclusion reduces bone regenerative capability of PRP<sup>38–42</sup>; hence, the PRF and PRF–FBG complex could be considered less potent than expected in bone regeneration.

Although PRF showed no positive effects on bone regeneration in this study, interestingly, the combination with RGD synergistically augmented the regenerative effects of PRF. A possible explanation of this phenomenon may be that osteoblasts and their precursor cells attached to the RGD-motif are more sensitive to growth factors and/or are protected from proinflammatory cytokines (PRF and PRF–FBG complex do not contain live leukocytes because these materials were once frozen for storage). Alternatively, FBG particles may function as growth factor carriers and delay the

release of growth factors. However, further molecular analyses are required to clarify this mechanism.

## CONCLUSIONS

The shortage of appropriate glass tubes is apparently an inconvenience for PRF users. To solve this impasse, many PRF users who do not have access to suitable high-quality glass tubes intend to use plastic tubes coated with microscopic silica particle films for examination of coagulation activity. The safety and suitability of such plastic tubes are not guaranteed for PRF therapy in most cases. Our proposed plastic tubes containing FBG enable us to prepare safe and implantable PRF clots, and the combinatorial PRF clots are more effective at bone regeneration than PRF or FBG alone are.

## DISCLOSURE

T. Hiratsuka and A. Azuma are employees of FUJIFILM Co. Ltd. All other authors have no conflict of interest relevant to this publication.

## REFERENCES

1. Nakamura K, Iwazawa R, Yoshioka Y. Introduction to a new cell transplantation platform via recombinant peptide petaloid pieces and its application to islet transplantation with mesenchymal stem cells. *Transpl Int* 2016;29(9):1039–1050.
2. Nakamura K, Tabata Y. A new fluorescent imaging of renal inflammation with RCP. *J Control Release* 2010;148(3):351–358.
3. Kawase T. Platelet-rich plasma and its derivatives as promising bioactive materials for regenerative medicine: Basic principles and concepts underlying recent advances. *Odontology* 2015;103:126–135.
4. Comert Kilic S, Gungormus M, Parlak SN. Histologic and histomorphometric assessment of sinus-floor augmentation with beta-tricalcium phosphate alone or in combination with pure-platelet-rich plasma or platelet-rich fibrin: A randomized clinical trial. *Clin Implant Dent Relat Res* 2017;19(5):959–967.
5. Miron RJ, Zucchelli G, Pikos MA, Salama M, Lee S, Guillemette V, Fujioka-Kobayashi M, Bishara M, Zhang Y, Wang HL, Chandad F, Nacopoulos C, Simonpieri A, Aalam AA, Felice P, Sammartino G, Ghanaati S, Hernandez MA, Choukroun J. Use of platelet-rich fibrin in regenerative dentistry: A systematic review. *Clin Oral Investig* 2017;21(6):1913–1927.
6. Al-Hamed FS, Tawfik MA, Abdelfadil E, Al-Saleh MAQ. Efficacy of platelet-rich fibrin after mandibular third molar extraction: A systematic review and meta-analysis. *J Oral Maxillofac Surg* 2017;75(6):1124–1135.
7. Castro AB, Meschi N, Temmerman A, Pinto N, Lambrechts P, Teughels W, Quirynen M. Regenerative potential of leucocyte- and platelet-rich fibrin. Part B: Sinus floor elevation, alveolar ridge preservation and implant therapy. A systematic review. *J Clin Periodontol* 2017;44(2):225–234.
8. Hartshorne J, Gluckman H. A comprehensive clinical review of platelet rich fibrin (PRF) and its role in promoting tissue healing and regeneration in dentistry. Part II: Preparation, optimization, handling and application, benefits and limitations of PRF. *Int Dent* 2016;6:34–48.
9. Kratz A, Stanganelli N, Van Cott EM. A comparison of glass and plastic blood collection tubes for routine and specialized coagulation assays: A comprehensive study. *Arch Pathol Lab Med* 2006;130(1):39–44.
10. Margolis J. Glass surface and blood coagulation. *Nature* 1956;178(4537):805–806.
11. Rapaport SI, Aas K, Owren PA. The increased coagulability of plasma exposed to glass. *Scand J Clin Lab Invest* 1954;6(1):82–83.
12. Toyoda T, Isobe K, Stujino T, Koyata Y, Ohyagi F, Watanabe T, Nakamura M, Kitamura Y, Okudera H, Nakata K Kawase T Direct activation of platelets by addition of CaCl<sub>2</sub> leads coagulation of platelet-rich plasma. *Int J Implant Dent*. 2018;4(1):23.
13. Kawase T, Watanabe T, Okuda K. Platelet-rich plasma and its derived platelet concentrates: What dentists involved in cell-based regenerative therapy should know. *Nihon Shishubyou Gakkai Kaishi* 2017;59(2):68–76. in Japanese.
14. Yoshioka Y, Maekawa T, Azuma A. Our challenge for developing regenerative medicine materials using recombinant peptide technology - possibility as a bone re-generative materials. *Biochem Clin* 2016;31(10):61–65. in Japanese.
15. Watanabe T, Isobe K, Suzuki T, Kawabata H, Nakamura M, Tsukioka T, Okudera T, Okudera H, Uematsu K, Okuda K, Nakata K, Kawase T. An evaluation of the accuracy of the subtraction method used for determining platelet counts in advanced platelet-rich fibrin and concentrated growth factor preparations. *Dent J* 2017;5(1):7.
16. Kitamura Y, Watanabe T, Nakamura M, Isobe K, Kawabata H, Uematsu K, Okuda K, Nakata K, Tanaka T, Kawase T. Platelet counts in insoluble platelet-rich fibrin clots: A direct method for accurate determination. *Front Bioeng Biotechnol* 2018;6:4.
17. Matsui R. Development of Terudermis, collagen-based artificial dermis and Teruplug, collagen-based material for extraction sockets. *J Japanese Assoc Regen Dent* 2008;6(1):9–20.
18. Kawase T, Tanaka T. An updated proposal for terminology and classification of platelet-rich fibrin. *Regen Therap* 2017;7:80–81.
19. Isobe K, Watanabe T, Kawabata H, Kitamura Y, Okudera T, Okudera H, Uematsu K, Okuda K, Nakata K, Tanaka T, Kawase T. Mechanical and degradation properties of advanced platelet-rich fibrin (A-PRF), concentrated growth factors (CGF), and platelet-poor plasma-derived fibrin (PPTF). *Int J Implant Dent* 2017;3(1):17.
20. Kawase T, Kamiya M, Kobayashi M, Tanaka T, Okuda K, Wolff LF, Yoshie H. The heat-compression technique for the conversion of platelet-rich fibrin preparation to a barrier membrane with a reduced rate of biodegradation. *J Biomed Mater Res B Appl Biomater* 2014;103(4):825–831.
21. Kobayashi M, Kawase T, Horimizu M, Okuda K, Wolff LF, Yoshie H. A proposed protocol for the standardized preparation of PRF membranes for clinical use. *Biologicals* 2012;40(5):323–329.
22. Isobe K, Suzuki M, Watanabe T, Kitamura Y, Suzuki T, Kawabata H, Nakamura M, Okudera T, Okudera H, Uematsu K, Nakata K, Tanaka T, Kawase T. Platelet-rich fibrin prepared from stored whole-blood samples. *Int J Implant Dent* 2017;3(1):6.
23. Kobayashi M, Kawase T, Okuda K, Wolff LF, Yoshie H. In vitro immunological and biological evaluations of the angiogenic potential of platelet-rich fibrin preparations: A standardized comparison with PRP preparations. *Int J Implant Dent* 2015;1(1):31.
24. Masuki H, Okudera T, Watanabe T, Suzuki M, Nishiyama K, Okudera H, Nakata K, Uematsu K, Su CY, Kawase T. Growth factor and pro-inflammatory cytokine contents in platelet-rich plasma (PRP), plasma rich in growth factors (PRGF), advanced platelet-rich fibrin (A-PRF), and concentrated growth factors (CGF). *Int J Implant Dent* 2016;2(1):19.
25. Kawase T, Okuda K, Nagata M, Tsuchimochi M, Yoshie H, Nakata K. Non-invasive, quantitative assessment of the morphology of gamma-irradiated human mesenchymal stem cells and periosteal cells using digital holographic microscopy. *Int J Radiat Biol* 2016;92(12):796–805.
26. Kawase T, Uematsu K, Kamiya M, Nagata M, Okuda K, Burns DM, Nakata K, Yoshie H. Real-time quantitative polymerase chain reaction and flow cytometric analyses of cell adhesion molecules expressed in human cell-multilayered periosteal sheets in vitro. *Cytotherapy* 2014;16(5):653–661.
27. Kawase T, Okuda K, Burns DM. Immature human osteoblastic MG63 cells predominantly express a subtype 1-like CGRP receptor that inactivates extracellular signal response kinase by a cAMP-dependent mechanism. *Eur J Pharmacol* 2003;470(3):125–137.
28. Kawase T, Okuda K, Burns DM. Immature osteoblastic MG63 cells possess two calcitonin gene-related peptide receptor subtypes that respond differently to [Cys(Acm)(2,7)] calcitonin gene-related peptide and CGRP(8-37). *Am J Physiol Cell Physiol* 2005;289(4):C811–C818.
29. Horimizu M, Kawase T, Nakajima Y, Okuda K, Nagata M, Wolff LF, Yoshie H. An improved freeze-dried PRP-coated biodegradable material suitable for connective tissue regenerative therapy. *Cryobiology* 2013;66(3):223–232.
30. Chen W, Zhou H, Weir MD, Tang M, Bao C, Xu HH. Human embryonic stem cell-derived mesenchymal stem cell seeding on calcium

- phosphate cement-chitosan-RGD scaffold for bone repair. *Tissue Eng Part A* 2013;19(7–8):915–927.
31. Heller M, Kumar VV, Pabst A, Brieger J, Al-Nawas B, Kammerer PW. Osseous response on linear and cyclic RGD-peptides immobilized on titanium surfaces in vitro and in vivo. *J Biomed Mater Res A* 2018;106(2):419–427.
  32. Ryu JJ, Park K, Kim HS, Jeong CM, Huh JB. Effects of anodized titanium with Arg-Gly-asp (RGD) peptide immobilized via chemical grafting or physical adsorption on bone cell adhesion and differentiation. *Int J Oral Maxillofac Implants* 2013;28(4):963–972.
  33. Garg P, Mazur MM, Buck AC, Wandtke ME, Liu J, Ebraheim NA. Prospective review of mesenchymal stem cells differentiation into osteoblasts. *Orthop Surg* 2017;9(1):13–19.
  34. Janssens K, ten Dijke P, Janssens S, Van Hul W. Transforming growth factor-beta1 to the bone. *Endocr Rev* 2005;26(6):743–774.
  35. Javed F, Al-Askar M, Al-Rasheed A, Al-Hezaimi K. Significance of the platelet-derived growth factor in periodontal tissue regeneration. *Arch Oral Biol* 2011;56(12):1476–1484.
  36. Xie H, Cui Z, Wang L, Xia Z, Hu Y, Xian L, Li C, Xie L, Crane J, Wan M, Zhen G, Bian Q, Yu B, Chang W, Qiu T, Pickarski M, Duong LT, Windle JJ, Luo X, Liao E, Cao X. PDGF-BB secreted by preosteoclasts induces angiogenesis during coupling with osteogenesis. *Nat Med* 2014;20(11):1270–1278.
  37. Marcazzan S, Weinstein RL, Del Fabbro M. Efficacy of platelets in bone healing: A systematic review on animal studies. *Platelets* 2018;29(4):326–337.
  38. Anitua E, Zalduendo MM, Prado R, Alkhraisat MH, Orive G. Morphogen and proinflammatory cytokine release kinetics from PRGF-Endoret fibrin scaffolds: Evaluation of the effect of leukocyte inclusion. *J Biomed Mater Res A* 2015;103(3):1011–1020.
  39. Davis VL, Abukabda AB, Radio NM, Witt-Enderby PA, Clafshenkel WP, Cairone JV, Rutkowski JL. Platelet-rich preparations to improve healing. Part II: Platelet activation and enrichment, leukocyte inclusion, and other selection criteria. *J Oral Implantol* 2014;40(4):511–521.
  40. Kizil C, Kyritsis N, Brand M. Effects of inflammation on stem cells: Together they strive? *EMBO Rep* 2015;16(4):416–426.
  41. Kobayashi Y, Saita Y, Nishio H, Ikeda H, Takazawa Y, Nagao M, Takaku T, Komatsu N, Kaneko K. Leukocyte concentration and composition in platelet-rich plasma (PRP) influences the growth factor and protease concentrations. *J Orthop Sci* 2016;21(5):683–689.
  42. Xu Z, Yin W, Zhang Y, Qi X, Chen Y, Xie X, Zhang C. Comparative evaluation of leukocyte- and platelet-rich plasma and pure platelet-rich plasma for cartilage regeneration. *Sci Rep* 2017;7:43301.